

# Magnetic Frustration on a Kagomé Lattice in $R_3Ga_5SiO_{14}$ Langasites with $R = Nd, Pr$

P Bordet<sup>1</sup>, I Gelard<sup>1</sup>, K Marty<sup>1</sup>, A Ibanez<sup>1</sup>, J Robert<sup>2</sup>, V Simonet<sup>2</sup>, B Canals<sup>2</sup>, R Ballou<sup>2</sup>, P Lejay<sup>3</sup>

<sup>1</sup> Laboratoire de Cristallographie, CNRS, B.P. 166, 38042 Grenoble Cedex 9, France

<sup>2</sup> Laboratoire Louis Néel, CNRS, B.P. 166, 38042 Grenoble Cedex 9, France

<sup>3</sup> Centre de Recherches des Très Basses Températures, CNRS, B.P. 166, 38 042 Grenoble Cedex 9, France

E-mail: pierre.bordet@grenoble.cnrs.fr, ballou@grenoble.cnrs.fr

**Abstract.** In the  $R_3Ga_5SiO_{14}$  compounds, the network  $R$  of rare earth cations form well separated planes of corner sharing triangles topologically equivalent to a kagomé lattice. Powder samples and single crystals with  $R = Nd$  and  $Pr$  were prepared and magnetostatic measurements were performed under magnetic field up to 10 T in the temperature range from 1.6 K to 400 K. Analysis of the magnetic susceptibility at the high temperatures where only the quadrupolar term of the crystal electric field prevails, suggests that the  $Nd$  and  $Pr$  magnetic moments can be modeled as coplanar elliptic rotators perpendicular to the three fold axis of the crystal structure that interact antiferromagnetically. Nonetheless, a disordered phase that can be ascribed to geometric frustration persists down to the lowest temperature which is about 25 times smaller than the energy scale for the exchange interactions.

PACS numbers: 61.66-f, 75.50-y, 75.30-Gw, 75.10.Dg

Submitted to: *J. Phys.: Condens. Matter*

The langasite series, the prototype of which is the  $\text{La}_3\text{Ga}_5\text{SiO}_{14}$  compound (LGS), hence the acronym, belongs to a vast family of materials having the  $\text{Ca}_3\text{Ga}_2\text{Ge}_4\text{O}_{14}$  type structure [1]. These materials rapidly attracted a strong interest because they show piezoelectric properties with better electro-mechanical coupling and weaker impedance than quartz or lithium niobate and tantalate [2]. They can be grown as high quality large single crystals, mainly by the Czochralski method, and are now used in surface acoustic wave filters in telecommunication devices and high temperature sensors. Crystallizing in a non centrosymmetric structure they exhibit quadratic non linear optical and electrooptical properties which are also intensively investigated [3]. On the other hand, probably because the interest was focused on the striking piezoelectric properties, the magnetic behaviors of these materials have not been studied until now, although several compounds contain arrays of magnetic cations. We report herein the magnetostatic properties of  $\text{Nd}_3\text{Ga}_5\text{SiO}_{14}$  (NGS) and  $\text{Pr}_3\text{Ga}_5\text{SiO}_{14}$  (PGS), which are isostructural to LGS. Inspection of the crystal structure and analysis of the magnetic susceptibility show that these provide us with a rare opportunity for a thorough investigation of geometric frustration in kagomé magnets, all the more as large single crystals can be grown.

Geometric frustration is currently attracting strong attention for the numerous novel phenomena it might generate [4]. It is classically featured by macroscopic degeneracies which prevent magnetic order to set up, thus allowing for new states of matter and unconventional excitations to come out [5]. Unfortunately the materialization of these generally meets with difficulties because of secondary interactions (next neighbors or antisymmetric exchange and magnetoelastic interactions) or structural and stoichiometric imperfections, which induce ordering at low temperatures. Within the temperature range we considered, this is not the case with NGS and PGS.

Langasite type compounds crystallize in the trigonal space group  $P321$ , with lattice parameters  $a = b = 8.07 \text{ \AA}$  and  $c = 5.06 \text{ \AA}$  (for NGS). The structure given in Table 1 for NGS and shown in Fig.1 contains four crystallographically non-equivalent cation sites, and the general formula can be written as  $\text{A}_3\text{BC}_3\text{D}_2\text{O}_{14}$ . The A site (3e at  $(\approx 0.42 \ 0 \ 0)$ ) is 8-coordinated by oxygen anions forming a distorted square antiprism. The B site (1a at  $(0 \ 0 \ 0)$ ) is octahedrally coordinated. The A and B site coordination polyhedra share edges to form a layer at  $z = 0$ . The C site (3f at  $(\approx 0.76 \ 0 \ 1/2)$ ) and the D site (2d at  $(1/3 \ 2/3 \approx 0.53)$ ) are both in tetrahedral coordination, the C site being larger than the D one. The  $\text{CO}_4$  and  $\text{DO}_4$  tetrahedra share corners to form a layer centered at  $z = \frac{1}{2}$ , and are also connected to the (A, B) cation layers above and below via corner sharing. In the NGS and PGS compounds [2], the rare earth trivalent cations occupy the large A sites, while the  $\text{Ga}^{3+}$  cations occupy the B, C and half of the D sites. The  $\text{Si}^{4+}$  cations are localized in the remaining half of the D sites. In Fig.2, the structural arrangement of the magnetic rare earth cations in NGS and PGS is outlined. It is formed by planes of corner sharing triangles perpendicular to the c-axis and separated from each other by the layer of tetrahedral C and D sites. The triangles are equilateral by symmetry, being centered by a 3-fold axis passing through the O1 and the mixed D

**Table 1.** Structural parameters for  $\text{Nd}_3\text{Ga}_5\text{SiO}_{14}$  determined by single crystal X-ray diffraction on a Bruker-Nonius kappaCCD diffractometer ( $\text{AgK}\alpha$  radiation) on a sphere of 0.1 mm radius, cut from a crystal grown by the floating zone technique. Data refined using the SHELX software [6].  $R_1 = 0.0273$ ,  $wR_2 = 0.0495$ ,  $\text{GooF} = 1.059$ . Cell parameters  $a = 8.066(1)$  Å,  $c = 5.062$  Å. The Ga3/Si3 site is half occupied by each cation.

Atom	Site	X	Y	Z	$U_{\text{eq}}(\text{\AA}^2)$
Nd	3e	0.41809(2)	0	0	0.00856(2)
Ga1	1a	0	0	0	0.01092(9)
Ga2	3f	0.76479(4)	0	1/2	0.00887(8)
Ga3/Si3	2d	1/3	2/3	0.5350(2)	0.00706(8)
O1	2d	2/3	1/3	0.8042(8)	0.0158(6)
O2	6g	0.5341(4)	0.8514(3)	0.6916(6)	0.0201(4)
O3	6g	0.2236(4)	0.0771(4)	0.7610(5)	0.0194(4)

sites, and the intercationic distances are 4.18 Å for NGS and 4.21 Å for PGS. Exchange interactions are mediated by the O1 and O2 oxygen anions. For NGS, the Nd-O1-Nd angle is  $110^\circ$  with two equal Nd-O1 distances at 2.554 Å, and the Nd-O2-Nd angle is  $106.5^\circ$  with two Nd-O2 distances at 2.38 Å and 2.83 Å. Because of the lack of hexagonal symmetry, this is not an ideal kagomé lattice but considering only the shortest atom bridging interactions we get the same overall topology.

Powders of the NGS and PGS compounds have been prepared by solid state reactions of stoichiometric amounts of high purity oxides at  $1420^\circ\text{C}$  in air. X-ray powder diffraction patterns indicated that the samples were single phase and Rietveld refinements confirmed the crystal structures reported in Ref. [2]. Single crystals of size up to 40 mm in length by 5 mm in diameter were grown by the floating zone method using an image furnace, under a 99% Ar + 1%  $\text{O}_2$  atmosphere, at a growth rate of 10 mm/h [7]. Although it does not allow to grow very large crystals, this technique has the advantage of preventing a crucible pollution due to long crystal growth times at high temperature necessary for the Czochralsky or Bridgman techniques. Moreover the size of the grown crystal is large enough to allow probing the spatially resolved dynamic spin-spin correlations by inelastic triple axis neutron scattering [8]. The unit cell and crystallographic orientations were checked using Laue photographs. The structure of a small piece of a NGS crystal was re-determined using single crystal X-ray diffraction with a kappaCCD x-ray diffractometer using  $\text{AgK}\alpha$  radiation. The results are in good agreement with those listed in Table 1 and those reported in [2]. We shall emphasize that to the accuracy of the experiment, the Nd site is fully occupied and no substitution of another cation for  $\text{Nd}^{3+}$  is detected.

The magnetostatic properties of NGS and PGS were investigated on single crystals under magnetic field up to 10 T in the temperature range from 1.6 K to 400 K on a purpose-built magnetometer using the anti-Helmholz two-coil axial extraction method

and on a commercial Quantum Design MPMS SQUID magnetometer. We show in Fig.3 the magnetic isotherms measured on NGS at 1.6 K and 100 K when the magnetic field is applied parallel ( $\parallel$ ) and perpendicular ( $\perp$ ) to the three fold axis  $\vec{c}$  of the crystal structure. We also give details of the thermal variation of the inverses  $1/\chi_{\parallel}$  and  $1/\chi_{\perp}$  of the initial magnetic susceptibilities deduced from the initial slope of the magnetic isotherms measured at different temperatures and from the thermal variation of the magnetization measured under a magnetic field of 1 T for the same two field orientations with respect to the  $\vec{c}$  axis. Similar measurements on PGS are displayed in Fig.4. A large uniaxial magnetocrystalline anisotropy is evidenced in both compounds in the whole temperature range of the measurements with the  $\vec{c}$  axis as the magnetization axis at low temperature changing to a hard axis on increasing the temperature at about 33 K in NGS and 127 K in PGS. A smaller magnetocrystalline anisotropy in the plane perpendicular to the  $\vec{c}$  axis exists which however dwindles out rapidly on increasing the temperature.

Analysis of the magnetic susceptibility can easily be performed at high temperature (T) by limiting the expansion of the quantum statistical average of the component of the magnetization along a quantization axis  $\vec{\alpha}$  ( $M_{\alpha}$ ) to low orders in  $1/T$  as done in [9]

$$M_{\alpha} = \frac{1}{N} \sum_{i=1}^N \frac{CH_{\alpha}^i}{T} \left\{ 1 - \frac{1}{k_B T} \frac{Tr [V^i O_{2\alpha}^0(\vec{J})]}{J(J+1)(2J+1)} \right\} + O\left(\frac{1}{T^3}\right) \quad (1)$$

$N$  is the number of the ions in the crystal.  $C = g_J^2 \mu_B^2 J(J+1)/3k_B$  is the Curie constant.  $J = 9/2$  for  $Nd^{3+}$  ions and  $J = 4$  for  $Pr^{3+}$  ions.  $H_{\alpha}^i$  is the component along  $\vec{\alpha}$  of the magnetic field on the  $i$ -th ion, including molecular field contribution.  $V^i$  accounts for the crystal electric field potential on the  $i$ -th ion and can be expanded as

$$V^i = \sum_k \sum_{q=-k}^k (A_{k\alpha}^q)^i O_{k\alpha}^q(\vec{J}) \quad (2)$$

in terms of Stevens equivalent operators  $O_{k\alpha}^q(\vec{J})$  [10, 11].  $k \leq 2l = 6$  for f electrons ( $l = 3$ ). Using the following identity  $\ddagger$ ,

$$\begin{aligned} Tr [O_{k\alpha}^q(\vec{J}) O_{2\alpha}^0(\vec{J})] &= Tr [(3J_{\alpha}^2 - (\vec{J})^2)^2] \delta_{k,2} \delta_{q,0} \\ &= \frac{1}{5} J(J+1)(2J+1)(2J-1)(2J+3) \delta_{k,2} \delta_{q,0} \end{aligned} \quad (3)$$

equation (1) is considerably simplified and allows to deduce the inverse of the initial uniform magnetic susceptibility  $\chi_{\alpha}$  along  $\vec{\alpha}$  as

$$\frac{1}{\chi_{\alpha}} \approx \frac{1}{C} \left\{ T - \theta + \frac{(2J-1)(2J+3)}{5k_B} \frac{1}{N} \sum_{i=1}^N (A_{2\alpha}^0)^i \right\} \quad (4)$$

where the paramagnetic Néel temperature  $\theta < 0$  accounts for the antiferromagnetic exchange interactions. The  $(A_{2\alpha}^0)^i$  coefficients are deduced from the crystal symmetry

$\ddagger$  This identity is derived on observing that the product  $\mathcal{D}_k \times \mathcal{D}_l$  of two irreducible representations  $\mathcal{D}_k$  and  $\mathcal{D}_l$  of the rotation group  $SO(3)$  contains the trivial representation  $\mathcal{D}_0$  solely if  $k = l$  and that the trace of  $O_{k\alpha}^q(\vec{J}) O_{l\alpha}^m(\vec{J})$  cancels unless  $q = -m$  since under a rotation  $\omega$  about the  $\vec{\alpha}$  axis this product is multiplied by  $e^{-i(q+m)\omega}$ .

at the  $i$ -th ion position, which consists of only a two fold axis :  $\vec{Z}^i = \vec{a}$  for the ion at  $(x \ 0 \ 0)$ ,  $\vec{Z}^i = \vec{b}$  for the ion at  $(0 \ x \ 0)$  and  $\vec{Z}^i = \vec{u} = \vec{a} + \vec{b}$  for the ion at  $(-x \ -x \ 0)$ , where  $x = 0.41809(2)$  for NGS (see Table 1). On choosing  $\vec{Z}^i$  as the quantization axis, adopting the three fold  $\vec{c}$  axis as the common  $\vec{Y}$  axis for all the ions and completing with the appropriate  $\vec{X}^i$  axis so that  $(X^i, Y, Z^i)$  forms a right handed frame,  $V^i$  writes  $B_2^0 O_{2Z}^0(\vec{J}) + B_2^2 O_{2Z}^2(\vec{J}) +$  terms of order 4 and 6 in  $k$ , where  $B_2^0$  and  $B_2^2$  do not depend on the  $i$ -th ion since, with respect to the  $(X^i, Y, Z^i)$  frame, the same crystal environment is seen by the  $i$ -th ion. We deduce on rotating the Stevens operators [12] that

$$\frac{1}{N} \sum_{i=1}^N (A_{2\parallel}^0)^i = -\frac{1}{2}(B_2^0 + B_2^2) \quad (5)$$

$$\frac{1}{N} \sum_{i=1}^N (A_{2\perp}^0)^i = \frac{1}{4}(B_2^0 + B_2^2) \quad (6)$$

We observe first that  $\chi_{\perp}$  does not depend upon the orientation of  $\vec{a}$  within the plane perpendicular to  $\vec{c}$ , which means that the in-plane anisotropy observed at low temperature should arise from higher order terms in the crystal electric field potential. In NGS, a linear fit of  $1/\chi_{\perp}$  above 100 K and of  $1/\chi_{\parallel}$  above 300 K using the slope fitted from  $1/\chi_{\perp}$  yields a paramagnetic Néel temperature  $\theta = -52$  K, an effective moment  $\mu_{\text{eff}} = 3.77 \mu_B$ , close to the value of the  $\text{Nd}^{3+}$  free ion, and a quadrupolar electric field parameter  $(B_2^0 + B_2^2)/k_B = -6.35$  K. No such quantitative analysis is possible in PGS because the temperatures at which  $1/\chi_{\parallel}$  and  $1/\chi_{\perp}$  are linear and parallel to each other are beyond the experimental range, but negative  $\theta$  and  $(B_2^0 + B_2^2)/k_B$  should be expected. As a matter of fact  $(B_2^0 + B_2^2) < 0$  in both NGS and PGS since  $\chi_{\parallel} < \chi_{\perp}$  at high temperature.

We computed both  $B_2^0$  and  $B_2^2$  for NGS in a point charge model considering the eight oxygen anions coordinating the  $\text{Nd}^{3+}$  ion and forming a distorted square antiprism around it. Generally the as-computed absolute values differ significantly from the actual ones, but the  $B_k^q/B_k^0$  ratios are better determined and a much greater confidence should be put on them. We get  $B_2^2/B_2^0 \approx 3/2$ , which suggests that the Nd magnetic moments behave at high temperature most probably as coplanar rotators perpendicular to  $\vec{c}$  with an orientational preference along the  $\vec{X}^i$  axis for the  $i$ -th ion within the  $(\vec{X}^i, Y)$  plane. A more complex behavior should occur at lower temperature where higher order terms of the crystal electric field compete with the quadrupolar one.

A fact of outmost importance was that, although finite values of the paramagnetic Néel temperature  $\theta$  are deduced, no anomaly is detected in the magnetic susceptibilities of both NGS and PGS indicating that a disordered phase would persist down to the lowest temperature despite antiferromagnetic interactions of one order of magnitude larger in energy scale. An elastic neutron scattering test experiment was performed using a powder sample of NGS on the D20 high flux diffractometer at the Institut Laue Langevin § that confirms the absence of any magnetic ordering. As evidenced in Fig.5

no increase in the Bragg intensity nor emergence of new Bragg intensity are observed on the neutron pattern on decreasing the temperature from 100 K down to 2 K.

In short, geometric frustration in  $Nd_3Ga_5SiO_{14}$  (NGS) and  $Pr_3Ga_5SiO_{14}$  (PGS) appears to inhibit condensation into a Néel phase and to favor a disordered phase down to the lowest temperature. We recently performed inelastic neutron scattering experiment on both polycrystals and single crystals evidencing liquid like dynamical spin-spin correlations with unusual dispersive features [8]. As from the present study of NGS and PGS, we expect that the series of  $R_3Ga_5SiO_{14}$  compounds with the other rare earth R should show valuable magnetic behaviors inherent to geometric frustration. As such they are of as much interest as from their piezoelectric properties.

## Acknowledgments

We thank the Institut Laue Langevin (ILL, Grenoble, France) for providing us with beam time for the neutron scattering experiment.

## References

- [1] Mill B V, Butashin A V, Kodzhabagyan G G, Belokonova, E L and Belov N V 1982 *Dokl. Akad. Nauk SSSR* **264** (6) 1395
- [2] Iwataki T, Ohsato H, Tanaka K, Morokoshi H, Sato J, and Kawasaki K 2001 *J. Eur. Cer. Soc.* **21** 1409
- [3] Xin Y, Jiyang W, Huaijin Z, Shaojun Z, Rongjiang H and Tingxiou C 2002 *Jpn. J. Appl. Phys.* **41** 7419
- [4] Ramirez A P 2001 *Handbook of Magnetic Materials* vol 13 ed. K. H. J. Buschow (Elsevier, New York) pp 423-520
- [5] Lhuillier C and Misguich G 2001 *High magnetic fields. Applications in condensed matter physics and spectroscopy* ed. C. Berthier, L.P. Levy, G. Ramirez (Springer-Verlag, Berlin) pp 161-190
- [6] Sheldrick G M 1997 *SHELX97 Programs for Crystal Structure Analysis* (Release 97-2). University of Göttingen, Germany.
- [7] Lejay P et al., in preparation.
- [8] Robert J, Simonet V, Canals B, Ballou R, Bordet P, Gelard I, Ibanez A, Lejay P, Ollivier J, Stunault A 2006 *Proc. Int. Conf. on Neutron scattering (Sidney, 2005)*; *Physica B* at press  
Robert J et al. in preparation.
- [9] Boutron P 1969 *J. de Phys. (Paris)* **30** 413
- [10] Stevens K W H 1952 *Proc. Roy. Soc. (London)* A **65** 209
- [11] Hutchings M T 1964 *Solid State Physics* vol 16 ed. F. Seitz and D. Turnbull (Academic, New York) pp 227-273
- [12] Rudowicz C 1985 *J. Phys. C: Solid State Phys.* **18** 1415



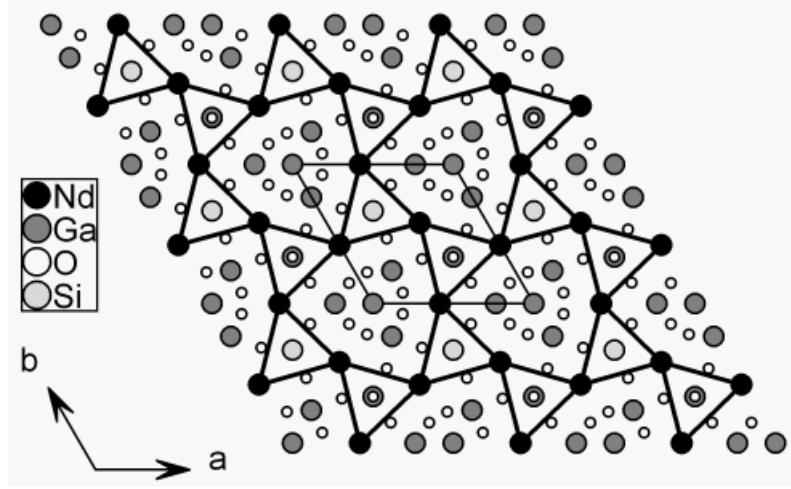


**Figure 2.** Atomic arrangement of  $\text{Nd}_3\text{Ga}_5\text{SiO}_{14}$  projected along the  $c$ -axis. The full lines linking the  $\text{Nd}^{3+}$  cations enhance the magnetic net topologically equivalent to a kagomé lattice.

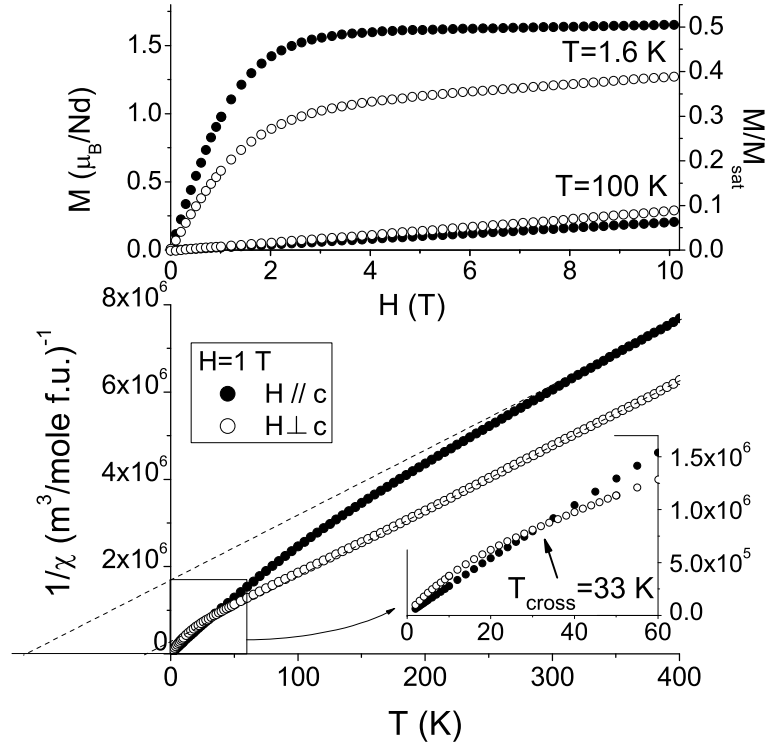


**Figure 3.** Magnetostatic data measured on a NGS single crystal under magnetic field parallel ( $\parallel$ ) and perpendicular ( $\perp$ ) to the three fold axis  $\vec{c}$ . Top : Magnetic isotherms at 1.6 K and 100 K. Bottom : Thermal variation of the inverses  $1/\chi_{\parallel}$  and  $1/\chi_{\perp}$  of the magnetic susceptibilities. The dashed lines stand for high temperature linear extrapolations for each field direction. Inset : zoom on the cross-over of  $1/\chi_{\parallel}$  and  $1/\chi_{\perp}$ .



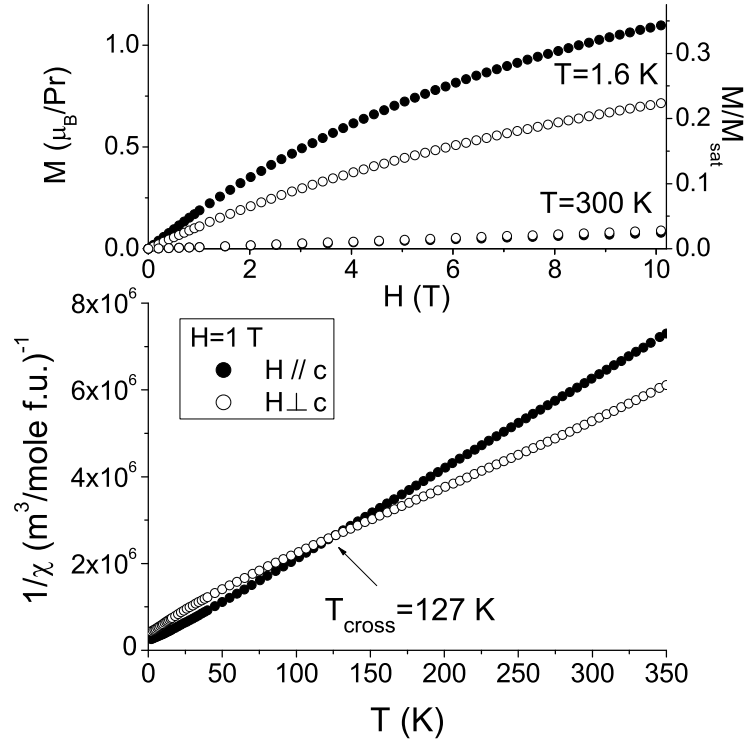


**Figure 4.** Magnetostatic data measured on a PGS single crystal under magnetic field parallel ( $\parallel$ ) and perpendicular ( $\perp$ ) to the three fold axis  $\vec{c}$ . Top : Magnetic isotherms at 1.6 K and 100 K. Bottom : Thermal variation of the inverses  $1/\chi_{\parallel}$  and  $1/\chi_{\perp}$  of the magnetic susceptibilities.

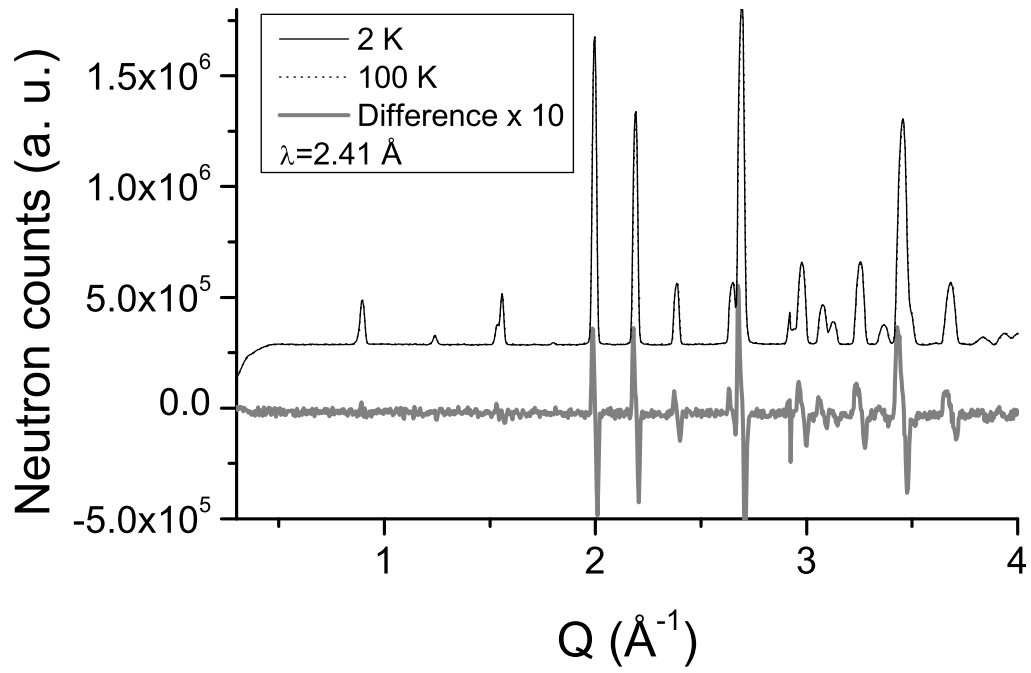


**Figure 5.** Neutron patterns collected at 100 K and 2 K from a powder sample of NGS and difference pattern multiplied by 10. The consecutive positive and negative intensities are due to thermal expansion.